

BKP states in the inclusive gluon production

M.Braun

Department of high-energy physics,
University of S. Petersburg, 198904 S. Petersburg, Russia

March 2010

Abstract Inclusive cross-section for gluon production is calculated by the dispersion technique in the NLO in the perturbative QCD with a large number of colours. The found cross-section coincides with the one derived in the dipole picture. No trace of the BKP states is found.

1 Introduction

In the perturbative QCD the inclusive gluon production is one of the most important observables, which can be directly compared to the experimental data. Applied to interaction with heavy nuclei it was first studied in [1] using the standard AGK rules and neglecting emission from the triple pomeron vertex. Later Yu. Kovchegov and K.Tuchin derived the single inclusive cross-section from the dipole picture [2]. Their expression contained an extra term as compared to [1] which was shown to correspond to emission from the triple-pomeron vertex [3]. However recently J.Bartels, M.Salvadore and G.-P. Vacca performed a new derivation [4] based on the dispersion approach, which studies discontinuities of amplitudes in various s -channels, the BFKL-Bartels (BB) technique [5], [6]. Their results are different from the previous ones in [2]. They contain new terms of a complicated structure, which seem to involve the so-called BKP states, higher pomerons composed of 3 and 4 reggeized gluons. Presence of such states will inevitably make calculations of the inclusive cross-section much more difficult (if possible at all), since their wave functions depend on many variables and are unknown at present. So the problem to understand the origin of the difference in the two derivations is quite important.

It may be that after all the initial physical picture in the two approaches is different. In the BB picture one is studying discontinuities of the standard Feynman diagrams in the Regge kinematics. In the Kovchegov-Tuchin (KT) picture gluon emission occurs due to eikonal scattering of fast quarks and gluons passing through the nucleus with instantaneous interactions with its components. So the first task in the study of the difference between the two results is to compare the initial expressions, which combine into the final inclusive cross-section. If they are different then in fact the two pictures are physically different and the difference in the resulting cross-sections is natural.

Actually the difference between the two pictures starts from the next-to-leading order in $\alpha_s \ln s$ (NLO) and originates from the contribution of one extra gluon softer than the observed gluon. One can prove that in this order the tree diagrams which describe single and double gluon emission identically coincide in these two pictures. The inclusive cross-section also includes diagrams with loops formed by the gluon softer than the observed one. In our previous paper [7] we were able to demonstrate that for single gluon emission and single interaction with the target contributions from such loops also identically coincide in the BFKL and the Kovchegov-Tuchin techniques. In the BFKL approach the mentioned loop generates the Regge trajectory of the exchanged gluon and thus is responsible for gluon reggeization. Our results showed that gluon reggeization is in fact realized by the loop contributions to the emission during eikonal scattering. More complicated loop diagrams with two or three interactions with the target also appear in the inclusive cross-section in the NLO. They are numerous and their full study is still far from being accomplished. However comparison of a relatively small subset of such diagrams, distinguished by their special dependence on the observed gluon momentum and polarization shows that their contribution again fully coincides in the two formalisms. So it seems almost certain that the physical pictures described by the BB and KT formalisms are fully equivalent and one may expect the inclusive cross-sections derived in these approaches to be completely identical.

The equations derived in [4] for the inclusive cross-section in the BB formalism are quite complicated and not at all transparent. One cannot exclude that in their solution all contributions which seem to be additional as compared to the KT result in fact cancel, so that in the end the two cross-sections indeed coincide. In this paper, to study this point, we directly compare the two cross-sections in the NLO, at which, as mentioned, the additional contribution starts in [4].

Our results show that the cross-sections described by the equations derived in the BB approach in [4] and in the KT approach in [2] completely coincide. So indeed all the additional contributions from the BKP intermediate states cancel.

The paper is organized as follows. In the next section we consider the inclusive cross-section in the KT approach in the first two orders. Section 3 is dedicated to a general overview of the inclusive cross-section in the BB approach and the relevant diagrammatic rules. Several next sections are devoted to direct calculations of various contributions to the cross-sections in the two possible target configurations, the so-called diffractive and double cut ones. In Sec 10 we collect our results to find the final inclusive cross-section in the next-to-leading order in the BB approach and compare it with the KT approach. In Section 11 we draw some conclusions. A few details concerning presentation of the KT cross-section in terms of BB diagrams are given in the Appendix 1. An essential identity for the BFKL pomeron wave function is derived in the Appendix 2.

2 Inclusive gluon production in KT approach

The KT expression for the inclusive gluon production cross-section was formulated in [4] in the framework of the dipole picture and uses the coordinate space formalism. However it can

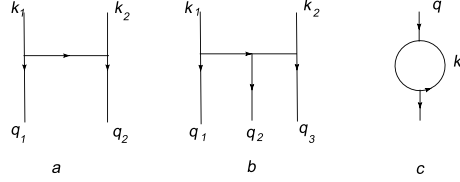


Figure 1: The Lipatov (a) and Bartels (b) kernels.

be directly reformulated in the BB language in the momentum space using results obtained in [3] and [8]. We shall use the momentum space formulation to facilitate the final comparison of the KT and BB cross-sections.

In the BB language contributions are described by a set of diagrams defined in the transverse momentum space and constructed from effective Lipatov and Bartels kernels, V and W correspondingly, illustrated in Fig. 1a, b and explicitly given by

$$V(q_1, q_2 | k_1, k_2) = \frac{(k_1 + k_2)^2}{k_1^2 k_2^2} - \frac{q_1^2}{k_1^2 (k_1 - q_1)^2} - \frac{q_2^2}{k_2^2 (k_2 - q_2)^2} \quad (1)$$

and

$$W(q_1, q_2, q_3 | k_1, k_2) = \frac{(k_1 + k_2)^2}{k_1^2 k_2^2} - \frac{(q_1 + q_2)^2}{k_1^2 (k_2 - q_3)^2} - \frac{(q_2 + q_3)^2}{k_2^2 (k_1 - q_1)^2} + \frac{q_2^2}{(k_1 - q_1)^2 (k_2 - q_3)^2}. \quad (2)$$

They also involve the gluon Regge trajectory Fig. 1c defined by the integral

$$\omega(q) = -g^2 N_c \frac{1}{2} \int \frac{d^2 k}{8\pi^3} \frac{q^2}{k^2 (q - k)^2}. \quad (3)$$

In this language the total contribution to the inclusive cross-section splits into two parts: emission from the upper pomeron and from the first splitting vertex. For scattering on two centers this generates three sets of diagrams shown in Fig. 2. The first two diagrams correspond to emission from the upper pomeron with the following splitting (Fig.2,1) or with the second term in the expansion of the Glauber expression for the state to be used as the initial state for the evolution in the Balitsky-Kovchegov equation (Fig.2,2). The third term (Fig. 2,3) corresponds to emission from the vertex. In the leading order (LO) the diagram in Fig. 2,1 gives no contribution and the two others reduce to the same diagram shown in Fig. 3. It has been demonstrated in [3] that this LO contribution is exactly reproduced by the sum of all relevant diagrams in the BB approach.

In the NLO the KT cross-section is represented by a sum of diagrams shown in Fig. 4. To simplify, we consider quarks both as the projectile and the two targets. It will inevitably introduce some infrared singularities into the cross-section, which are however irrelevant for our purpose, since the impact factors for the participants factorize. To simulate the colorless quark-antiquark loops we average on the quark colours and add a similar contribution from the antiquark. To economise on notations in the end we shall suppress all necessary integrations,

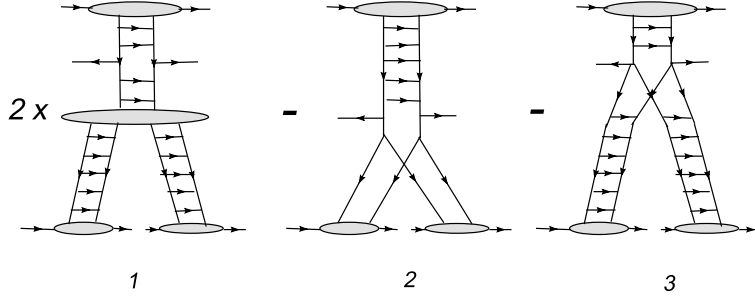


Figure 2: Inclusive gluon production in the KT approach. Emission from the upper pomeron (1+2) and from the vertex (3).

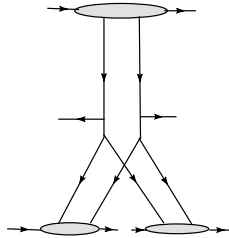


Figure 3: The KT inclusive cross-section in LO

obvious powers of the coupling constant g and number of colours N_c and factorized projectile and target factors.

In Fig. 4 and all the following we show all partons with solid lines. The upper and bottom lines refer to the projectile and target quarks respectively. Vertical lines refer to reggeons (just longitudinal gluons in our approximation). The rest horizontal lines describe interaction kernels V and W and correspond to real transverse gluons. The three lines of diagrams in Fig. 4 correspond to the three terms in Fig. 2. To the first and last lines one should add similar diagrams which make the contribution symmetric in the two lower legs.

To write down the corresponding analytic expressions we denote the observed gluon transverse momentum and rapidity as k_1 and y_1 and those of the softer gluon k_2 and y_2 with $y_2 \ll y_1$ and $k_{2+} \ll k_{1+}$. The transverse momenta of the final reggeons coupled to the first target quark are denoted q_1 and q_2 . For the inclusive cross-section on a heavy nucleus the total momentum transferred to the nucleus components is small. So we take $q_1 + q_2 = 0$. The transverse momenta of the second pair of final reggeons are q_3 and q_4 with $q_3 + q_4 = 0$. One is to perform integrations over momenta of the unobserved emitted gluon k_2 and final quark lines q_1 and q_2 . We omit the factors which arise from the final quark lines, so that the final factor which appears in the inclusive cross-section is

$$2\alpha_s N_c \int \frac{dk_{2+}}{k_{2+}} \frac{d^2 k_2}{4\pi^2} \frac{d^2 q_1}{(2\pi)} \frac{d^2 q_4}{(2\pi)}. \quad (4)$$

This factor will also be suppressed and assumed to be added to our expressions in the end. One has also to take into account that the pomeron wave function vanishes when the two

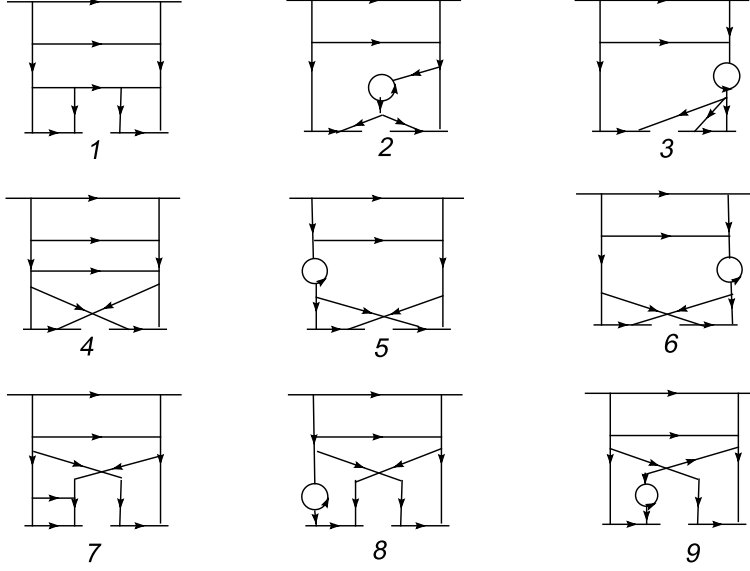


Figure 4: The KT inclusive cross-section in NLO. Vertical lines denote reggeons. Uppermost and lowermost horizontal lines denote the colliding quarks. Middle lines denote the observed gluon with momentum k_1 (upper) and virtual softer gluon with momentum k_2

reggeons are located at the same point. In the momentum space it means that integrated over its relative momentum the pomeron vanishes. As a result all contributions which do not depend either on q_1 or on q_4 vanish after integrations over q_1 and q_4 . This allows to drop diagrams like Fig 4,3.

In terms of V , W and ω the NLO contribution to the KT cross-section is given by the sum

$$\frac{8\pi^3 d\sigma^{KT}}{dy d^2k_1 d^2b} \equiv I^{KT} = \sum_{i=1}^3 I_i^{KT}, \quad (5)$$

where the three terms I_i^{KT} , $i = 1, 2, 3$, correspond to contributions from diagrams in Fig. 2, and are given by (see Appendix for some details)

$$I_1^{KT} = 2V(k_2, -k_2|k_2 + k_1, -k_2 - k_1)W(q_1, -q_{14}, q_4|k_2, -k_2) \\ + 2\omega(q_{14})\left(V(q_1, -q_1|q_1 + k_1, -q_1 - k_1) + V(-q_4, q_4| -q_4 + k_1, q_4 - k_1)\right), \quad (6)$$

$$I_2^{KT} = -V(q_{14}, -q_{14}|q_{14} + k_2, -q_{14} - k_2)V(q_{14} + k_2, -q_{14} - k_2|q_{14} + k_2 + k_1, -q_{14} - k_2 - k_1) \\ + 2\omega(q_{14})V(q_{14}, -q_{14}|q_{14} + k_1, -q_{14} - k_1), \quad (7)$$

$$I_3^{KT} = V(q_{14} + k_2, -q_{14} - k_2|q_{14} + k_2 + k_1, -q_{14} - k_2 - k_1)\left(-V(q_1, -q_1|q_1 + k_2, -q_1 - k_2) \right. \\ \left. - V(q_4, -q_4|q_4 + k_2, -q_4 - k_2)\right) \\ + 2V(q_{14}, -q_{14}|q_{14} + k_1, -q_{14} - k_1)\left(\omega(q_1) + \omega(q_4)\right), \quad (8)$$

where $q_{14} = q_1 + q_4$. As indicated these expressions are to be taken with a common factor (4).

For future comparison with the BB picture it is convenient to reexpress these contributions via function

$$F(q, p) \equiv (q|p) = \frac{q^2}{p^2(q-p)^2} = (q|q-p) = (-q|-p). \quad (9)$$

Then one has

$$V(q_1, -q_1|q_1 + k_2, -q_1 - k_2) = -2(q_1, k_2), \quad (10)$$

$$\omega(q_1) = -\frac{1}{2}(q_1|k_2) \quad (11)$$

and the NLO contributions to the KT cross-section become

$$I_1^{KT} = -4(k_2|-k_1)(q_{14}|q_1 - k_2) + 2(q_{14}|k_2)\left((q_1|-k_1) + (q_4|k_1)\right), \quad (12)$$

$$I_2^{KT} = -2(q_{14}|-k_2)\left(2(q_{14} + k_2|-k_1) - (q_{14}|-k_1)\right), \quad (13)$$

$$I_3^{KT} = -2\left((q_1|-k_2) + (q_4|-k_2)\right)\left(2(q_{14} + k_2|-k_1) - (q_{14}|-k_1)\right). \quad (14)$$

It is understood that in these expressions k_1 is fixed, k_2 is integrated over as indicated in (4) and q_1 and q_2 are integrated over with the pomeron wave functions in the lowest approximation. It is these expressions that we shall compare with the BB cross-section.

3 BB cross-section, generalities

In the BB approach the inclusive gluon production is derived from the contribution to the total cross-section by fixing the momentum and rapidity of the observed gluon in the intermediate state. The total cross-section on two centers is given by a set of all reggeon diagrams connecting the projectile with the two targets and including interaction between reggeons either by the Lipatov kernel V , conserving their number, or by the Bartels kernel W , increasing their number.

Comparison with the KT approach requires to take identical weights in the momentum integrations and also appropriate normalizations of impact factors for the projectile and the two targets in the triple pomeron contribution. The weight adopted in the BB formalism is $1/(8\pi^3)$ different from the standard one $1/(4\pi^2)$ for the Fourier transform. Taking into account that each momentum integration but one is accompanied by factor g^2 we can pass to the standard weight $1/(4\pi^2)$ substituting

$$g^2 \rightarrow \tilde{g}^2 = \frac{g^2}{2\pi} = 2\alpha_s. \quad (15)$$

(The lifted extra integration with weight $1/(8\pi^3)$ leads to the inclusive cross-section normalized as in (5)). In the following substitution (15) is assumed to be made. To properly normalize the impact factors in the triple pomeron contribution we take into account the

relation between the functions Φ and Ψ which give the sum of fan diagrams and also between the projectile impact factors χ and D in the KT and BB approaches correspondingly ¹

$$\Phi = -\tilde{g}^2\Psi, \quad \chi = -\frac{1}{\tilde{g}^2}D. \quad (16)$$

Suppression of all impact factors in the KT approach then translates into division of the contribution of BB triple pomeron diagrams by $1/\tilde{g}^2$ (the minus sign goes due to the fact that the diagrams themselves refer to the triple cut contribution and should be taken with the opposite sign for the amplitude). As a result the final expressions will be accompanied by the same factor (4).

All the diagrams can be separated by the initial number of reggeons to describe transitions from 2 to 4 reggeons, 3 to 4 reggeons and 4 to 4 reggeons. In the NLO the diagrams can include either two interactions (V or W) or one interaction and an insertion of the gluon Regge trajectory ω , which transforms the gluon into reggeon. In the last case the resulting contribution gives a part of terms which correspond to the BFKL evolution of the final pomerons, the other part given by the BFKL interaction V inside the pair of legs. The sum of all such terms can be calculated in the straightforward manner noting that in the LO the sum of all BB diagrams gives exactly the KT cross-section, that is twice the contribution from Fig. 3. In the NLO the BFKL evolution of the legs will give twice the contribution I_3^{KT} .

$$I_1^{BB} = 2I_3^{KT}. \quad (17)$$

The rest diagrams can in their turn be split into two sets depending on how the 4 final gluon legs are coupled to the two target quarks. The first possibility is that counting from the left the first pair of gluons (momenta q_1 and q_2) are coupled to the first target quark and the second pair (momenta q_3 and q_4) are coupled to the second target quark. We call such configuration diffractive. An alternative configuration is when the first and last gluons (momenta q_3 and q_4) are coupled to the second target quark and the middle pair (momenta q_1 and q_2) are coupled to the first quark. We call this configuration 'double cut' for reasons to be explained presently. The third possible configuration (not neighbouring gluons coupled to each target quark) is damped in the heavy nucleus.

The inclusive cross-section corresponds to fixing the observed gluon in the intermediate state (that is in some interaction V or W). The result is to be interpreted as a product of a certain production amplitude by another production amplitude taken complex conjugate. This corresponds to cutting the diagram across the real intermediate states. In both configurations this cut may be done in two different ways. In the diffractive configuration the cut either does not pass through the target quarks at all, the diffractive (D) contribution, which corresponds to the physical diffractive case, or passes through one of the target quarks, single diffractive (SD) contribution. One can show that the D and SD contribution of the same diagram enter with the opposite sign. In the double cut contribution the cut can pass

¹This relation was first established in [9], where however the correct weight factor in the momentum integrations was not taken into account nor the fact that the triple pomeron vertex for the amplitude was twice smaller and of the opposite sign.

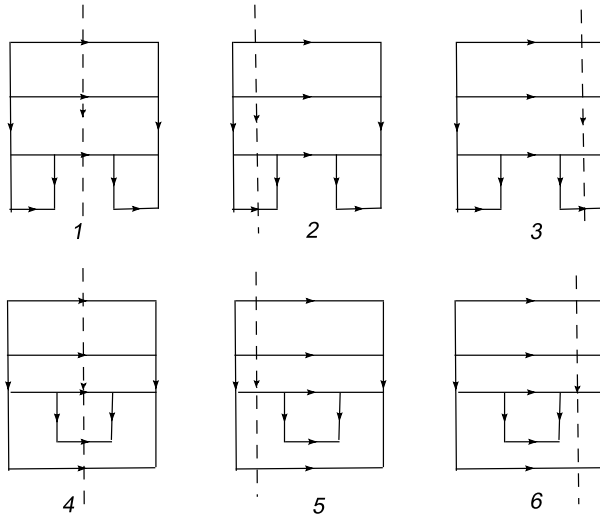


Figure 5: The diagrams in the BB approach which correspond to Fig 4,1 in the diffractive (1,2,3) and double cut (4,5,6) configurations. (See notations in Fig. 4.)

either through both the target quark (DC contribution, hence the name) or again through only one of the target quarks (single double cut (SDC) contribution). The DC contribution enters with factor 2 and the SDC contribution with factor -1 .

The final factor for each contribution is determined taking into account the sum over colours, which can be taken directly from the diagram noting that each 3 gluon vertex contributes f^{abc} with gluon colours a, b and c taken anticlockwise.

To see how these rules work consider the diagrams of the same type as Fig. 4,1 for the KT amplitude in the preceding section. In the BB framework one finds a set of diagrams shown in Fig. 5.

We recall that all partons are shown by simple solid lines. The upper and bottom lines refer to the projectile and target quarks respectively. Vertical lines refer to reggeons (just longitudinal gluons in our approximation). The rest horizontal lines describe interaction kernels V and W and correspond to real transverse gluons. Colour summation for the diagram gives factor $-N_c^5$, or just -1 suppressing the common N_c^5 .

The DC contribution cancels with two SDC contributions. The sign of the D contribution is reversed by the two SD contributions. Writing the D contribution in terms of V and W and reversing the sign we get the term corresponding to the contribution of the diagram in Fig. 4,1 for the KT cross-section but with a twice smaller coefficient

$$I_2^{BB} = -2(k_2| - k_1)(q_{14}|q_1 - k_2). \quad (18)$$

We are left with the sum of all BB diagrams I_R^{BB} excluding Fig. 5 and all diagrams with ω insertions and inserions of V between the gluon legs connected to a given target quark. They will be studied in the next two sections.

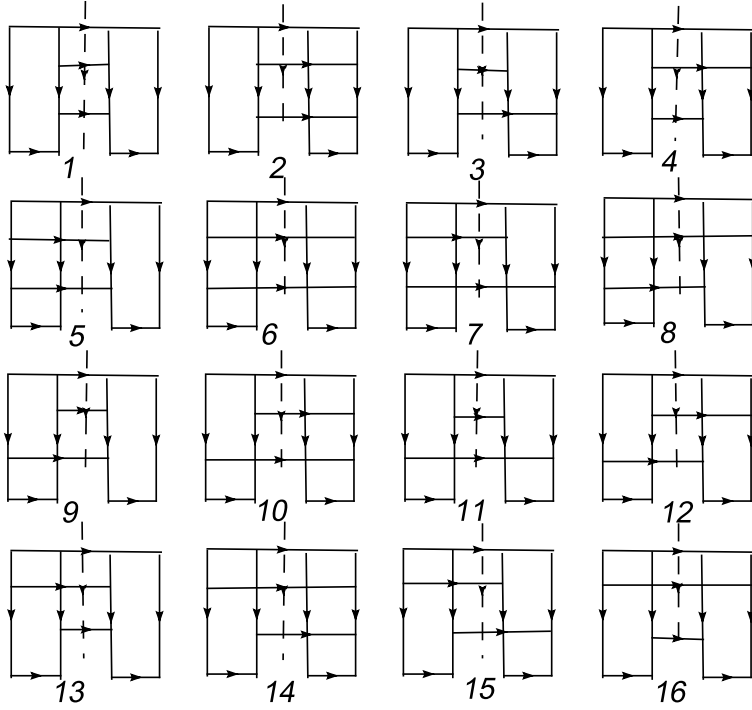


Figure 6: Feynman diagrams $4 \rightarrow 4$ for the inclusive cross-section in the diffractive configuration. (See notations in Fig. 4.)

4 Diffractive $4 \rightarrow 4$ diagrams (case 1)

All 16 diagrams cut in the middle are shown in Fig. 5. One can split the whole set in three subsets depending on the position of the upper horizontal line corresponding to the observed gluon with the larger rapidity.

The first set is formed by the diagrams (1),(3),(9) and (11). Here the upper gluon connects the two inner reggeized gluons. As a result there will be no contribution from the same diagrams with one of the target quarks cut, the single diffractive (SD) contribution, since such a cut does not contain the observed gluon. Therefore contributions from this set remain as such.

The second set is formed by the diagrams (6),(8), (14) and (16). Here the upper gluon connects the two outside reggeized gluons. So it will be present in both SD cuts passing through the left and right target quarks. Since each SD contribution is equal to the middle cut contribution but has the opposite sign, in the sum the contribution from this set will change sign.

Finally we have the third set of diagrams (2),(5), (4),(7),(10), (12), (13), and (15) in which the observed gluon appears only in one of the two SD contributions. So the contribution from this set cut in the middle will be completely cancelled by the SD contribution.

Now we are going to demonstrate that the contributions from the first and second set cancel in the sum. To do this we have to write explicitly the integrand in k_2 , q_1 and q_4 in

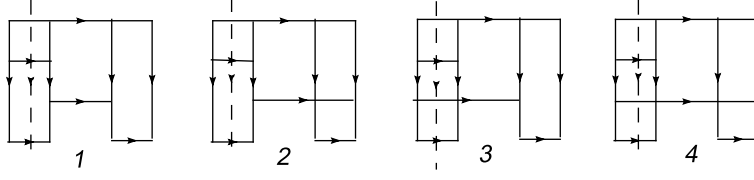


Figure 7: Single cut diagrams in the diffractive configuration. To the shown diagrams complex conjugate ones are to be added. (See notations in Fig. 4.)

each of the relevant diagrams. Taking into account their colour factors we find the following expressions for the diagrams from the 1st set.

$$\begin{aligned}
(1) &= -\frac{1}{8}V(q_2, q_3|q_2 + k_2, q_3 - k_2)V(q_2 + k_2, q_3 - k_2|q_2 + k_2 + k_1, q_3 - k_2 - k_1), \\
(3) &= +\frac{1}{8}V(q_2, q_4|q_2 + k_2, q_4 - k_2)V(q_2 + k_2, q_3|q_2 + k_2 + k_1, q_3 - k_1), \\
(9) &= +\frac{1}{8}V(q_1, q_3|q_1 + k_2, q_3 - k_2)V(q_2, q_3 - k_2|q_2 + k_1, q_3 - k_2 - k_1), \\
(11) &= -\frac{1}{8}V(q_1, q_4|q_1 + k_2, q_4 - k_2)V(q_2, q_3|q_2 + k_1, q_3 - k_1),
\end{aligned}$$

where in fact $q_2 = -q_1$ and $q_3 = -q_4$.

The diagrams in the second set have the integrands

$$\begin{aligned}
(6) &= -\frac{1}{8}V(q_1, q_4|q_1 + k_2, q_4 - k_2)V(q_1 + k_2, q_4 - k_2|q_1 + k_2 + k_1, q_4 - k_2 - k_1), \\
(8) &= +\frac{1}{8}V(q_1, q_3|q_1 + k_2, q_3 - k_2)V(q_1 + k_2, q_4|q_1 + k_2 + k_1, q_4 - k_1), \\
(14) &= +\frac{1}{8}V(q_2, q_4|q_2 + k_2, q_4 - k_2)V(q_1, q_4 - k_2|q_1 + k_1, q_4 - k_2 - k_1), \\
(16) &= -\frac{1}{8}V(q_2, q_3|q_2 + k_2, q_3 - k_2)V(q_1, q_4|q_1 + k_1, q_4 - k_1).
\end{aligned}$$

We observe that (6), (8), (14) and (16) are obtained from (1), (3), (9) and (11) respectively by the substitutions $q_1 \leftrightarrow q_2$ and $q_3 \leftrightarrow q_4$. However these substitutions do not change the result after integration over q_1 and q_4 , so that the diagrams have in fact the same values. However, as mentioned, the SD contribution in fact changes sign of the diagrams in the second set. So in the sum they cancel with the first set.

Thus the $4 \rightarrow 4$ diagrams shown in Fig. 6 cancel in the sum and give no contribution to the inclusive cross-section. Additional 8 diagrams in the SD configuration are shown in Fig. 7 plus their complex conjugate.

The corresponding integrands are

$$(1) = -\frac{1}{8}V(q_2, q_3|q_2 + k_2, q_3 - k_2)V(q_1, q_2 + k_2|q_1 + k_1, q_2 + k_2 - k_1),$$

$$\begin{aligned}
(2) &= +\frac{1}{8}V(q_2, q_4|q_2 + k_2, q_4 - k_2)V(q_1, q_2 + k_2|q_1 + k_1, q_2 + k_2 - k_1), \\
(3) &= +\frac{1}{8}V(q_1, q_3|q_1 + k_2, q_3 - k_2)V(q_1 + k_2, q_2|q_1 + k_2 + k_1, q_2 - k_1), \\
(4) &= -\frac{1}{8}V(q_1, q_4|q_1 + k_2, q_4 - k_2)V(q_1 + k_2, q_2|q_1 + k_2 + k_1, q_2 - k_1).
\end{aligned}$$

The change $q_3 \leftrightarrow q_4$ shows that (1)+(2)=(3)+(4)= 0. So the conclusion is that all $4 \rightarrow 4$ diffractive contribution cancels out.

To accommodate our notations to cover all cases we present our results in the form

$$V(q_1, q_2|q_1 + k_2, q_4 - k_2) \cdot X$$

for diffractive and double cut contributions, to be taken with coefficient +1 in the total cross-section and

$$V(q_1, q_2|q_1 + k_2, q_4 - k_2) \cdot Y$$

for all single cut contributions, to be taken with coefficient -1 in the total cross-section. We have found that in case 1

$$X_1 = Y_1 = 0. \quad (19)$$

5 Diffractive $2 \rightarrow 4$ diagrams (case 2)

Diagrams $2 \rightarrow 4$ are shown in Fig. 8, cut in the middle. One finds that diagrams (2) and (3) are cancelled with one of the SD contributions, that with the cut left target quark. Diagrams (4) and (7) are cancelled with the SD contribution corresponding to the cut right target quark. Diagram (1), which summed with the two SD contributions changes its sign, has already been studied in Sec. 3. So we are left with diagrams (5), (6), (8), (9) and 12 SD diagrams.

The integrands for diagrams (5), (6), (8) and (9) are

$$\begin{aligned}
(5) &= -\frac{1}{4}V(q_2, q_3|q_2 + k_2, q_3 - k_2)W(q_1, q_2 + q_3, q_4|q_1 + q_2 + k_1 + k_2, q_4 + q_3 - k_1 - k_2), \\
(6) &= +\frac{1}{4}V(q_2, q_4|q_2 + k_2, q_4 - k_2)W(q_1, q_2 + q_3 + k_2, q_4 - k_2|q_1 + q_2 + k_1 + k_2, q_4 + q_3 - k_1 - k_2), \\
(8) &= +\frac{1}{4}V(q_1, q_3|q_1 + k_2, q_3 - k_2)W(q_1 + k_2, q_2 + q_3 - k_2, q_4|q_1 + q_2 + k_1 + k_2, q_4 + q_3 - k_1 - k_2), \\
(9) &= -\frac{1}{4}V(q_1, q_4|q_1 + k_2, q_4 - k_2)W(q_1 + k_2, q_2 + q_3, q_4 - k_2|q_1 + q_2 + k_1 + k_2, q_4 + q_3 - k_1 - k_2).
\end{aligned}$$

Using invariance under substitutions $q_1 \leftrightarrow q_2$ and $q_3 \leftrightarrow q_4$ we transform the Lipatov kernel in the first three term to the common form $V(q_1, q_4|q_1 + k_2, q_4 - k_2)$. In the sum of these diagrams we then get

$$D_{2 \rightarrow 4} = (5) + (6) + (8) + (9) = V(q_1, q_4|q_1 + k_2, q_4 - k_2) \cdot X_2, \quad (20)$$

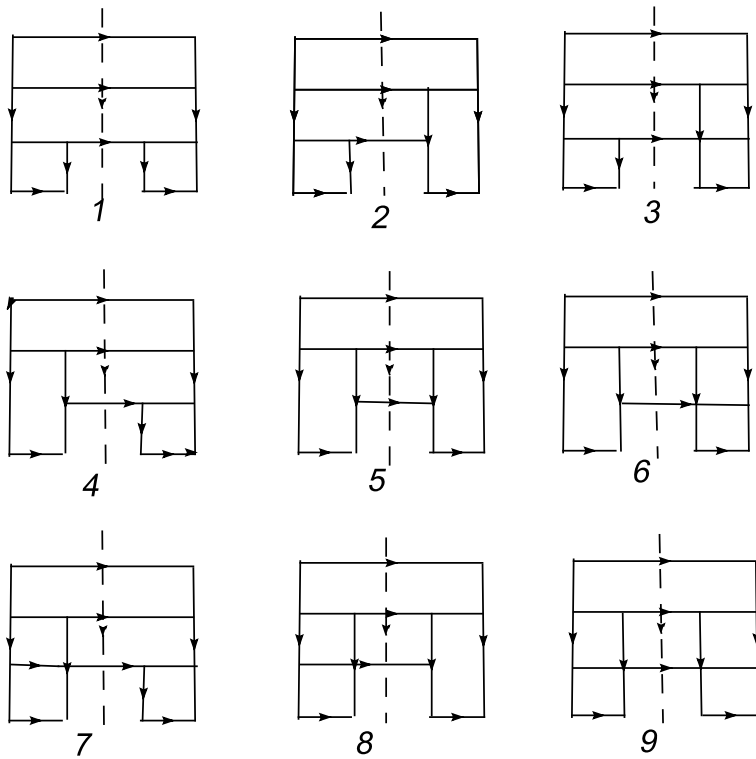


Figure 8: Feynman diagrams 2 \rightarrow 4 for the inclusive cross-section in the diffractive configuration. (See notations in Fig. 4.)

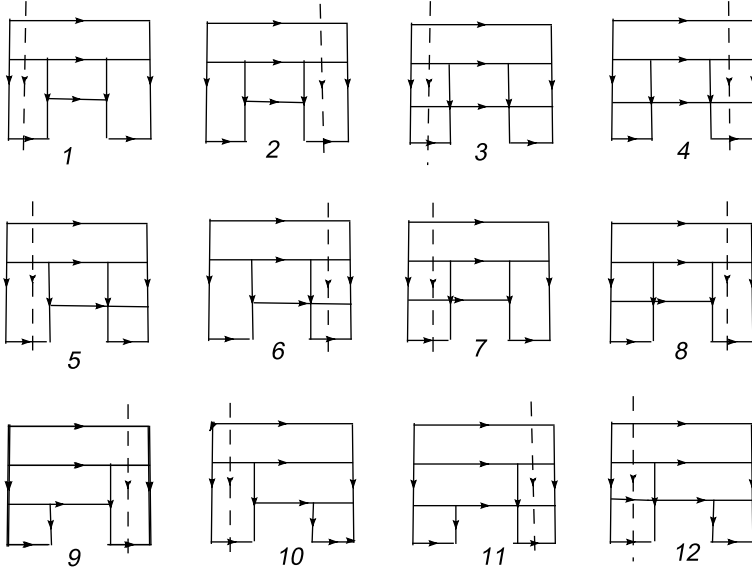


Figure 9: Feynman diagrams 2 \rightarrow 4 for the inclusive cross-section in the diffractive configuration with one of the target quarks cut. (See notations in Fig. 4.)

where

$$\begin{aligned}
X_2 = & -\frac{1}{4}W(q_2, q_1 + q_4, q_3|q_1 + q_2 + k_1 + k_2, q_3 + q_4 - k_1 - k_2) \\
& +\frac{1}{4}W(q_2, q_1 + q_3 + k_2, q_4 - k_2|q_1 + q_2 + k_1 + k_2, q_3 + q_4 - k_1 - k_2) \\
& +\frac{1}{4}W(q_1 + k_2, q_2 + q_4 - k_2, q_3|q_1 + q_2 + k_1 + k_2, q_3 + q_4 - k_1 - k_2) \\
& -\frac{1}{4}W(q_1 + k_2, q_2 + q_3, q_4 - k_2|q_1 + q_2 + k_1 + k_2, q_3 + q_4 - k_1 - k_2). \quad (21)
\end{aligned}$$

Now we consider the SD terms. The corresponding 12 diagrams are presented in Fig.9. The integrands are

$$\begin{aligned}
(1) = (2) = & -\frac{1}{4}V(q_2, q_3|q_2 + k_2, q_3 - k_2)W(q_1, q_2 + q_3, q_4|q_1 + k_1, q_2 + q_3 + q_4 - k_1), \\
(5) = (8) = & +\frac{1}{4}V(q_2, q_4|q_2 + k_2, q_4 - k_2)W(q_1, q_2 + q_3 + k_2, q_4 - k_2|q_1 + k_1, q_2 + q_3 + q_4 - k_1), \\
(6) = (7) = & +\frac{1}{4}V(q_2, q_4|q_2 + k_2, q_4 - k_2)W(q_1, q_2 + q_3 + k_2, q_4 - k_2|q_1 + q_2 + q_3 + k_1 + k_2, q_4 - k_2 - k_1), \\
(3) = (4) = & -\frac{1}{4}V(q_1, q_4|q_1 + k_2, q_4 - k_2)W(q_1 + k_2, q_2 + q_3, q_4 - k_2|q_1 + k_1 + k_2, q_2 + q_3 + q_4 - k_1 - k_2), \\
(9) = (10) = & -\frac{1}{2}W(q_1, q_2, q_3|q_1 + q_2 + k_2, q_3 - k_2)W(q_1 + q_2 + k_2, q_3 - k_2, q_4|q_1 + q_2 + q_3 + k_1, q_4 - k_1), \\
(11) = (12) = & +\frac{1}{2}W(q_1, q_2, q_4|q_1 + q_2 + k_2, q_4 - k_2) \\
& W(q_1 + q_2 + k_2, q_3, q_4 - k_2|q_1 + q_2 + q_3 + k_1 + k_2, q_4 - k_2 - k_1).
\end{aligned}$$

In (1), (2), (5) – (8) we again transform the V -factor to the common form $V(q_1, q_4|q_1 + k_2, q_4 - k_2)$ using the symmetry under reflection $q_1 \rightarrow -q_1, q_4 \rightarrow -q_4$. In (9)-(12) we use $q_1 + q_2 = 0$ and the identity

$$W(q_1, -q_1, q_3|k_2, q_3 - k_2) = -V(-q_1, q_3| -q_1 + k_2, q_3 - k_2). \quad (22)$$

Then we get

$$(9) = (10) = \frac{1}{2}V(q_1, q_4|q_1 + k_2, q_4 - k_2)W(k_2, q_4 - k_2, q_3|q_4 + k_1, q_3 - k_1)$$

and

$$(11) = (12) = -\frac{1}{2}V(q_1, q_4|q_1 + k_2, q_4 - k_2)W(k_2, q_3, q_4 - k_2|q_3 + k_1 + k_2, q_4 - k_2 - k_1).$$

So we find

$$SD_{2 \rightarrow 4} = \sum_{j=1}^{12} (j) = V(q_1, q_4|q_1 + k_2, q_4 - k_2) \cdot Y_2, \quad (23)$$

where

$$\begin{aligned} Y_2 = & -\frac{1}{2}W(q_2, q_1 + q_4, q_3|q_2 + k_1, q_1 + q_3 + q_4 - k_1) \\ & -\frac{1}{2}W(q_1 + k_2, q_2 + q_3, q_4 - k_2|q_1 + k_1 + k_2, q_2 + q_3 + q_4 - k_1 - k_2) \\ & +\frac{1}{2}W(q_2, q_1 + q_3 + k_2, q_4 - k_2|q_2 + k_1, q_1 + q_3 + q_4 - k_1) \\ & +\frac{1}{2}W(q_2, q_1 + q_3 + k_2, q_4 - k_2|q_1 + q_2 + q_3 + k_1 + k_2, q_4 - k_1 - k_2) \\ & +W(k_2, q_4 - k_2, q_3|q_4 + k_1, q_3 - k_1) - W(k_2, q_3, q_4 - k_2|q_3 + k_1 + k_2, q_4 - k_1 - k_2). \end{aligned} \quad (24)$$

6 Diffractive $3 \rightarrow 4$ diagrams (case 3)

The 24 $3 \rightarrow 4$ diagrams are shown in Fig. 10 plus their complex conjugate.

One observes that the contributions from diagrams (1), and (7) are cancelled by the SD contributions coming from the cut right target quark and from diagrams (5), (6), (11) and (12) by the SD contribution from the cut left target quark. Diagrams (4) and (10) change sign by the two SD contributions from the cut left and right target quarks. Diagrams (2), (3), (8) and (9) remain as such.

Integrands for the remaining diagrams are

$$(2) = -\frac{1}{8}V(q_2, q_3|q_2 + k_2, q_3 - k_2)W(q_2 + k_2, q_3 - k_2, q_4|q_2 + k_1 + k_2, q_3 + q_4 - k_1 - k_2),$$

$$(3) = \frac{1}{8}V(q_2, q_4|q_2 + k_2, q_4 - k_2)W(q_2 + k_2, q_3, q_4 - k_2|q_2 + k_1 + k_2, q_3 + q_4 - k_1 - k_2),$$

$$(8) = \frac{1}{8}V(q_1, q_3|q_1 + k_2, q_3 - k_2)W(q_2, q_3 - k_2, q_4|q_2 + k_1, q_3 + q_4 - k_1 - k_2),$$

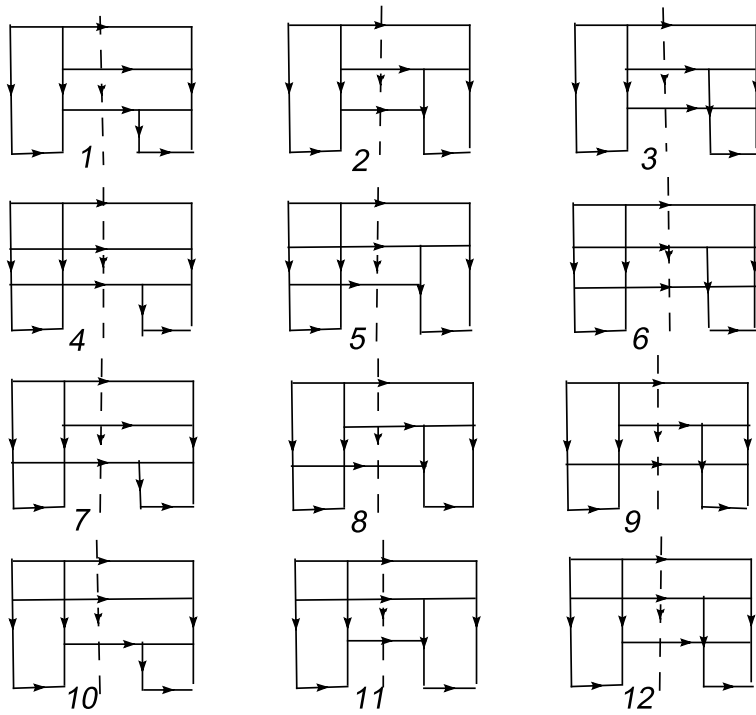


Figure 10: Feynman diagrams $3 \rightarrow 4$ for the inclusive cross-section in the diffractive configuration. To the shown diagrams one should add their complex conjugate ones. (See notations in Fig. 4.)

$$\begin{aligned}
(9) &= -\frac{1}{8}V(q_1, q_4|q_1 + k_2, q_4 - k_2)W(q_2, q_3, q_4 - k_2|q_2 + k_1, q_3 + q_4 - k_1 - k_2), \\
(4) &= -\frac{1}{4}W(q_1, q_3, q_4|q_1 + k_2, q_3 + q_4 - k_2)V(q_1 + k_2, q_3 + q_4 - k_2|q_1 + k_1 + k_2, q_3 + q_4 - k_1 - k_2), \\
(10) &= \frac{1}{4}W(q_2, q_3, q_4|q_2 + k_2, q_3 + q_4 - k_2)V(q_1, q_3 + q_4 - k_2|q_1 + k_1, q_3 + q_4 - k_1 - k_2).
\end{aligned}$$

For (4) and (10) we again use Eq.(22) and changing $q_4 \rightarrow -q_4$ find

$$\begin{aligned}
(4) &= \frac{1}{4}V(q_1, q_4|q_1 + k_2, q_4 - k_2)V(q_1 + k_2, -k_2|q_1 + k_1 + k_2, -k_1 - k_2), \\
(10) &= -\frac{1}{4}V(q_1, q_4|q_1 + k_2, q_4 - k_2)V(q_2, -k_2|q_2 + k_1, -k_1 - k_2).
\end{aligned}$$

Separating factor $V(q_1, q_4|q_1 + k_2, q_4 - k_2)$ in the rest of diagrams and doubling we obtain the total diffractive contribution from $3 \rightarrow 4$ transitions

$$D_{3 \rightarrow 4} = V(q_1, q_4|q_1 + k_2, q_4 - k_2) \cdot X_3, \quad (25)$$

where

$$\begin{aligned}
X_3 &= -\frac{1}{4}W(q_1 + k_1, q_4 - k_2, q_3|q_1 + k_1 + k_2, -k_1 - k_2) \\
&\quad + \frac{1}{4}W(q_1 + k_1, q_3, q_4 - k_2|q_1 + k_1 + k_2, -k_1 - k_2) \\
&\quad + \frac{1}{4}W(q_2, q_4 - k_2, q_3|q_2 + k_1, -k_1 - k_2) - \frac{1}{4}W(q_2, q_3, q_4 - k_2|q_1 + k_1, -k_1 - k_2) \\
&\quad + \frac{1}{2}V(q_1 + k_2, -k_2|q_1 + k_1 + k_2, -k_1 - k_2) - \frac{1}{2}V(q_2, -k_2|q_2 + k_1, -k_1 - k_2). \quad (26)
\end{aligned}$$

Now we pass to SD diagrams which remain after cancellation with the diffractive diagrams. They are 10 and are shown in Fig. 11. The integrands are

$$\begin{aligned}
(1) &= -\frac{1}{8}V(q_2, q_3|q_2 + k_2, q_3 - k_2)W(q_2 + k_2, q_3 - k_2, q_4|q_2 + q_3 + k_1, q_4 - k_1), \\
(2) &= \frac{1}{8}V(q_2, q_4|q_2 + k_2, q_4 - k_2)W(q_2 + k_2, q_3, q_4 - k_2|q_2 + q_3 + k_1 + k_2, q_4 - k_1 - k_2), \\
(3) &= \frac{1}{8}V(q_1, q_3|q_1 + k_2, q_3 - k_2)W(q_1 + k_2, q_3 - k_2, q_4|q_1 + q_3 + k_1, q_4 - k_1), \\
(4) &= -\frac{1}{8}V(q_1, q_4|q_1 + k_2, q_4 - k_2)W(q_1 + k_2, q_3, q_4 - k_2|q_1 + q_3 + k_1 + k_2, q_4 - k_1 - k_2), \\
(5) &= \frac{1}{8}V(q_1, q_3|q_1 + k_2, q_3 - k_2)W(q_2, q_3 - k_2, q_4|q_2 + q_3 + k_1 - k_2, q_4 - k_1), \\
(6) &= -\frac{1}{8}V(q_1, q_4|q_1 + k_2, q_4 - k_2)W(q_2, q_3, q_4 - k_2|q_2 + q_3 + k_1, q_4 - k_1 - k_2), \\
(7) &= -\frac{1}{8}V(q_2, q_3|q_2 + k_2, q_3 - k_2)W(q_1, q_3 - k_2, q_4|q_1 + q_3 + k_1 - k_2, q_4 - k_1), \\
(8) &= \frac{1}{8}V(q_2, q_4|q_2 + k_2, q_4 - k_2)W(q_1, q_3, q_4 - k_2|q_1 + q_3 + k_1, q_4 - k_1 - k_2),
\end{aligned}$$

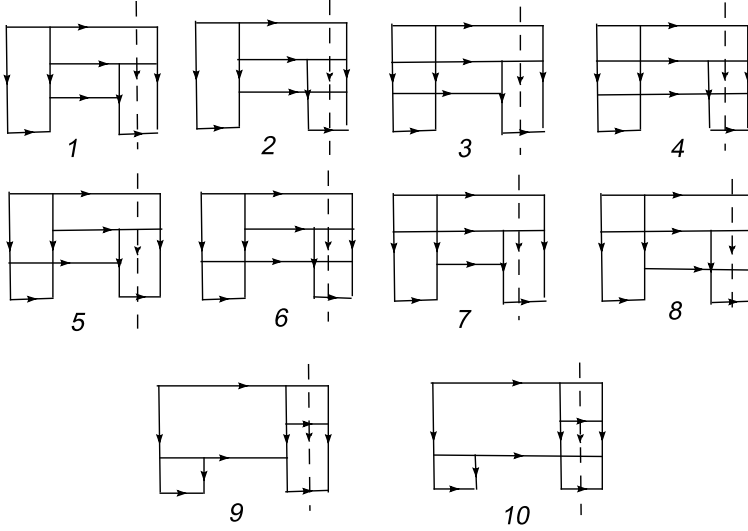


Figure 11: Feynman diagrams $3 \rightarrow 4$ for the inclusive cross-section in the diffractive configuration with one of the target quarks cut. (See notations in Fig. 4.)

$$(9) = -\frac{1}{4}W(q_1, q_2, q_3|q_1 + q_2 + k_2, q_3 - k_2)V(q_3 - k_2, q_4|q_3 + k_1 - k_2, q_4 - k_1),$$

$$(10) = \frac{1}{4}W(q_1, q_2, q_4|q_1 + q_2 + k_2, q_4 - k_2)V(q_3, q_4 - k_2|q_3 + k_1, q_4 - k_1 - k_2).$$

We observe that

$$(3) = -(1) \text{ with } q_1 \leftrightarrow q_2, \quad (4) = -(2) \text{ with } q_1 \leftrightarrow q_2,$$

$$(7) = -(5) \text{ with } q_1 \leftrightarrow q_2, \quad (8) = -(6) \text{ with } q_1 \leftrightarrow q_2.$$

Changing $q_3 \leftrightarrow q_4$ and $k_1 \rightarrow -k_1$ in (10) we also find $(9) = -(10)$. So the sum of all 8 diagrams is zero and the $SD_{3 \rightarrow 4}$ diagrams give no contribution : $Y_3 = 0$

7 Double cut (DC) $4 \rightarrow 4$ diagrams (case 4)

The eight $4 \rightarrow 4$ middle cut DC diagrams with non-zero colour factors are shown in Fig. 12. Of them 4 diagrams (2), (4), (6) and (8) are completely cancelled by the corresponding single cut contributions. We are left with 4 diagrams (1), (3), (5) and (7). Their direct calculations give the following integrands for the integrals over k_2 , q_1 and q_4

$$(1) = (3) = 2 \times \left(\frac{1}{8}\right)V(q_1, q_4|q_1 + k_2, q_4 - k_2)V(q_1 + k_2, q_2|q_1 + k_1 + k_2, q_2 - k_1),$$

$$(5) = (7) = -2 \times \left(\frac{1}{8}\right)V(q_2, q_4|q_2 + k_2, q_4 - k_2)V(q_1, q_2 + k_2|q_1 + k_1, q_2 + k_2 - k_1),$$

where the separated factor two comes from taking the double cut uncompensated by single cut contributions. A change $q_1 \leftrightarrow q_2$ in the second expression converts it into the first with

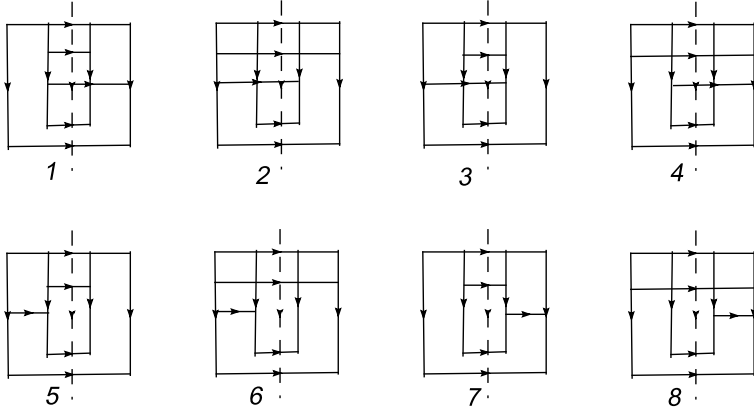


Figure 12: Feynman diagrams $4 \rightarrow 4$ for the inclusive cross-section in the double cut configuration. (See notations in Fig. 4.)

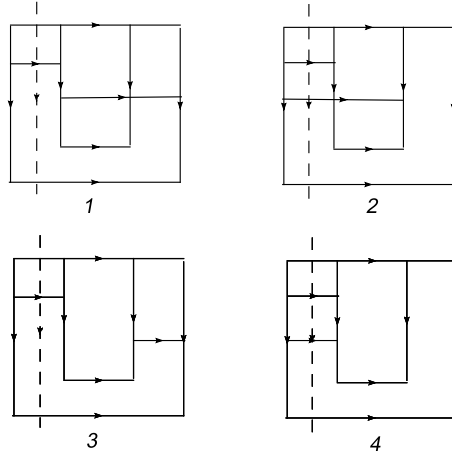


Figure 13: Single cut diagrams in the double cut configuration. To the shown diagrams their complex conjugate ones are to be added. (See notations in Fig. 4.)

the opposite sign. So $(1) + (5) = 0$ and the contribution from terms $4 \rightarrow 4$ shown in Fig. 12 is completely cancelled as in the diffractive configuration.

Additional 8 diagrams in the SD configuration are shown in Fig. 13 plus their complex conjugate.

The corresponding integrands are

$$(1) = \frac{1}{8}V(q_1, q_4|q_1 + k_2, q_4 - k_2)V(q_3, q_1 + k_2|q_3 + k_1, q_1 + k_2 - k_1),$$

$$(2) = \frac{1}{8}V(q_3, q_2|q_3 + k_2, q_2 - k_2)V(q_3 + k_2, q_1|q_3 + k_1 + k_2, q_1 - k_1),$$

$$(3) = -\frac{1}{8}V(q_2, q_4|q_2 + k_2, q_4 - k_2)V(q_3, q_1|q_3 + k_1, q_1 - k_1),$$

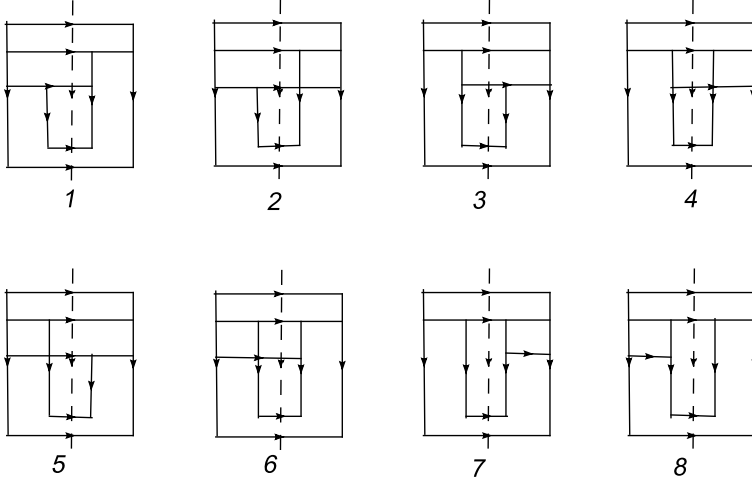


Figure 14: Feynman diagrams 2 \rightarrow 4 for the inclusive cross-section in the double cut configuration. (See notations in Fig. 4.)

$$(4) = -\frac{1}{8}V(q_3, q_1|q_3 + k_2, q_1 - k_2)V(q_3 + k_2, q_1 - k_2|q_3 + k_1 + k_2, q_1 - k_1 - k_2).$$

To separate the common factor $V(q_1, q_4|q_1 + k_2, q_4 - k_2)$ we change $q_1 \leftrightarrow q_2$, $q_3 \leftrightarrow q_4$ and $k_2 \rightarrow -k_2$ in (2), $q_2 \leftrightarrow q_1$ in (3) and $q_3 \leftrightarrow q_4$ and $k_2 \rightarrow -k_2$ in (4). Then we get

$$SDC_{4 \rightarrow 4} = 2\left((1) + (2) + (3) + (4)\right) = V(q_1, q_4|q_1 + k_2, q_4 - k_2) \cdot Y_4, \quad (27)$$

where

$$Y_4 = \frac{1}{4}V(q_3, q_1 + k_2|q_3 + k_1, q_1 + k_2 - k_1) + \frac{1}{4}V(q_4 - k_2, q_2|q_4 + k_1 - k_2, q_2 - k_1) \\ - \frac{1}{4}V(q_3, q_2|q_3 + k_1, q_2 - k_1) - \frac{1}{4}V(q_4 - k_2, q_1 + k_2|q_4 + k_1 - k_2, q_1 - k_1 + k_2). \quad (28)$$

8 DC 2 \rightarrow 4 diagrams (case 5)

8 relevant diagrams are shown in Fig. 14. Diagrams (1), (2), (3) and (5) have one corresponding single cut contribution, so that their initial coefficient 2 is reduced to unity. Diagrams (4), (6), (7) and (8) remain with the coefficient 2. The integrands obtained from the straightforward calculations are

$$(1) = (3) = -\frac{1}{2}W(q_3, q_1, q_2|q_3 + k_2, q_1 + q_2 - k_2) \\ W(q_3 + k_2, q_1 + q_2 - k_2, q_4|q_3 + k_1 + k_2, q_1 + q_2 + q_4 - k_1 - k_2), \\ (2) = (5) = \frac{1}{4}W(q_3, q_1, q_4|q_1 + q_3 + k_2, q_4 - k_2) \\ W(q_1 + q_3 + k_2, q_2, q_4 - k_2|q_1 + q_3 + k_1 + k_2, q_2 + q_4 - k_1 - k_2),$$

$$\begin{aligned}
(4) &= (6) = 2 \times \left(\frac{1}{4}\right) V(q_1, q_4 | q_1 + k_2, q_4 - k_2) \\
&W(q_3, q_1 + q_2 + k_2, q_4 - k_2 | q_1 + q_3 + k_1 + k_2, q_2 + q_4 - k_1 - k_2), \\
(7) &= (8) = -2 \times \left(\frac{1}{4}\right) V(q_2, q_4 | q_2 + k_2, q_4 - k_2) \\
&W(q_3, q_1 + q_2 + k_2, q_4 - k_2 | q_1 + q_3 + k_1, q_2 + q_4 - k_1).
\end{aligned}$$

The first and last expressions can be transformed to our standard form with factor $V(q_1, q_4, q_1 + k_2, q_4 - k_2)$ using Eq.(22) and the change $q_3 \leftrightarrow q_4$ and $k_2 \rightarrow -k_2$

$$(1) = (3) = \frac{1}{2} V(q_1, q_4 | q_1 + k_2, q_4 - k_2) W(q_4 - k_2, k_2, q_3 | q_4 + k_1 - k_2, q_3 - k_1 + k_2).$$

In the expression for (7) it is sufficient to change $q_1 \leftrightarrow q_2$. Contribution (2)=(5) cannot be transformed to the standard form with factor $V(q_1, q_4 | q_1 + k_2, q_4 - k_2)$ separated. However we shall see that this contribution is cancelled with a similar one coming from the single cut diagrams.

As a result the DC contribution from $2 \rightarrow 4$ transitions is

$$DC_{2 \rightarrow 4} = (1) + (3) + (4) + (6) + (7) + (8) = V(q_1, q_4 | q_1 + k_2, q_4 - k_2) \cdot X_5, \quad (29)$$

where

$$\begin{aligned}
X_5 &= W(q_4 - k_2, k_2, q_3 | q_4 + k_1 - k_2, q_3 - k_1 + k_2) \\
&+ W(q_3, q_1 + q_2 + k_2, q_4 - k_2 | q_1 + q_3 + k_1 + k_2, q_2 + q_4 - k_1 - k_2) \\
&- W(q_3, q_1 + q_2 + k_2, q_4 - k_2 | q_2 + q_3 + k_1, q_1 + q_4 - k_1).
\end{aligned} \quad (30)$$

Now we pass to single cut diagrams associated with the DC $2 \rightarrow 4$ diagrams (SDC $2 \rightarrow 4$ diagrams). The 12 SDC $2 \rightarrow 4$ diagrams are shown in Fig. 15. They are pairwise equal, so we have to study 6 different contributions. Calculations give the following integrands

$$\begin{aligned}
(1) = (3) &= -\frac{1}{2} W(q_3, q_1, q_2 | q_3 + k_2, q_1 + q_2 - k_2) W(q_3 + k_2, q_1 + q_2 - k_2, q_4 | q_1 + q_2 + q_3 + k_1, q_4 - k_1), \\
(2) = (6) &= \frac{1}{4} W(q_3, q_1, q_4 | q_1 + q_3 + k_2, q_4 - k_2) \\
&W(q_1 + q_3 + k_2, q_2, q_4 - k_2 | q_1 + q_2 + q_3 + k_1 + k_2, q_4 - k_1 - k_2), \\
(4) = (8) &= \frac{1}{4} V(q_1, q_4 | q_1 + k_2, q_4 - k_2) W(q_3, q_1 + q_2 + k_2, q_4 - k_2 | q_3 + k_1, q_1 + q_2 + q_4 - k_1), \\
(5) = (7) &= \frac{1}{4} V(q_1, q_4 | q_1 + k_2, q_4 - k_2) W(q_3, q_1 + q_2 + k_2, q_4 - k_2 | q_1 + q_2 + q_3 + k_1 + k_2, q_4 - k_1 - k_2), \\
(9) = (12) &= -\frac{1}{4} V(q_2, q_4 | q_2 + k_2, q_4 - k_2) W(q_3, q_1 + q_2 + k_2, q_4 - k_2 | q_3 + k_1, q_1 + q_2 + q_4 - k_1), \\
(10) = (11) &= -\frac{1}{4} V(q_2, q_4 | q_2 + k_2, q_4 - k_2) \\
&W(q_3, q_1 + q_2 + k_2, q_4 - k_2 | q_1 + q_2 + q_3 + k_1 + k_2, q_4 - k_1 - k_2).
\end{aligned}$$

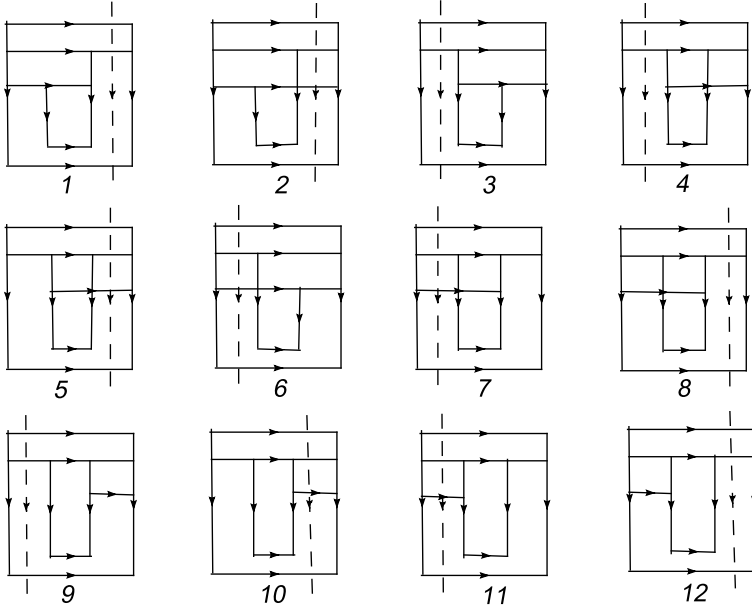


Figure 15: Feynman diagrams $2 \rightarrow 4$ for the inclusive cross-section with one of the target quarks cut associated with the double cut configuration. (See notations in Fig. 4.)

Changing $q_1 \leftrightarrow q_2$ we find that $(4) + (9) = (5) + (10) = 0$. So the total contribution reduces to $2(1) + 2(2)$. Contribution (1) can be transformed to the standard form. Using (22) and changing $q_3 \leftrightarrow q_4$ and $k_2 \rightarrow -k_2$ we find

$$(1) = (3) = \frac{1}{2}V(q_1, q_4|q_1 + k_2, q_4 - k_2)W(q_4 - k_2, k_2, q_3|q_4 + k_1, q_3 - k_1).$$

Now we demonstrate that contributions from $(2)+(6)$ cancel similar contributions $(2)+(5)$ from the $DC_{2 \rightarrow 4}$ diagrams. We make a change of the integration momentum $k_2 \rightarrow -k_2 - q_1$ in $SDC(2)$ to get

$$SDC(2) = -W(q_3, q_2, q_4|q_3 - k_2, q_1 + q_4 + k_2)$$

$$W(q_3 - k_2, q_2, q_1 + q_4 + k_2|q_2 + q_3 + k_1 - k_2, q_1 + q_4 - k_1 + k_2).$$

Change $q_3 \leftrightarrow q_4$ and $k_1 \rightarrow -k_1$ transforms $SDC(2)$ into $DC(2)$. Since they enter the inclusive cross-section with opposite signs, their contributions cancel.

As a result the only contribution left from the single cut diagrams $2 \rightarrow 4$ comes from the sum $(1)+(3)$

$$SDC_{2 \rightarrow 4} = (1) + (3) = V(q_1, q_4|q_1 + k_2, q_4 - k_2) \cdot Y_5, \quad (31)$$

where

$$Y_5 = W(q_4 - k_2, k_2, q_3|q_4 + k_1, q_3 - k_1). \quad (32)$$

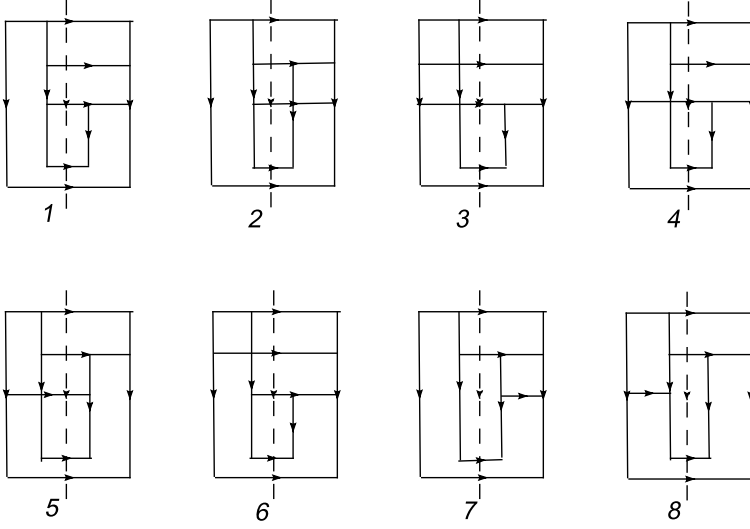


Figure 16: Feynman diagrams 3 \rightarrow 4 for the inclusive cross-section in the double cut configuration. Complex conjugate diagrams are to be added. (See notations in Fig. 4.)

9 DC 3 \rightarrow 4 diagrams (case 6)

The interference DC diagrams 3 \rightarrow 4 come in pairs. Half of them with non-zero colour coefficients are shown in Fig. 16 (8 diagrams). Of them diagrams (3) and (6) are completely cancelled by the associated single cut contributions. Diagrams (1) and (4) become half-wise cancelled by the single cut contribution and its coefficient 2 is reduced to unity. The rest 4 diagrams (2), (5), (7) and (8) remain with coefficient 2. Direct calculation gives the following integrands

$$(1) = -\frac{1}{4}W(q_1, q_2, q_4|q_1 + q_2 + k_2, q_4 - k_2)V(q_1 + q_2 + k_2, q_4 - k_2|q_1 + q_2 + k_1 + k_2, q_4 - k_1 - k_2),$$

$$(2) = 2 \times \left(\frac{1}{8}\right)V(q_1, q_4|q_1 + k_2, q_4 - k_2)W(q_1 + k_2, q_2, q_4 - k_2|q_1 + k_1 + k_2, q_2 + q_4 - k_1 - k_2),$$

$$(4) = \frac{1}{8}W(q_3, q_2, q_4|q_3 + k_2, q_2 + q_4 - k_2)V(q_1, q_2 + q_4 - k_2|q_1 + k_1, q_2 + q_4 - k_1 - k_2),$$

$$(5) = 2 \times \left(\frac{1}{8}\right)V(q_3, q_2|q_3 + k_2, q_2 - k_2)W(q_1, q_2 - k_2, q_4|q_1 + k_1, q_2 + q_4 - k_1 - k_2),$$

$$(7) = 2 \times \left(-\frac{1}{8}\right)V(q_2, q_4|q_2 + k_2, q_4 - k_2)W(q_1, q_2 + k_2, q_4 - k_2|q_1 + k_1, q_2 + q_4 - k_1),$$

$$(8) = 2 \times \left(-\frac{1}{8}\right)V(q_3, q_1|q_3 + k_2, q_1 - k_2)W(q_1 - k_2, q_2, q_4|q_1 + k_1 - k_2, q_2 + q_4 - k_1).$$

As before we transform all expressions except (4) to the standard form. In (1) we use Eq.(22) to find

$$(1) = \frac{1}{4}V(q_1, q_4|q_1 + k_2, q_4 - k_2)V(k_2, q_4 - k_2|k_1 + k_2, q_4 - k_1 - k_2).$$

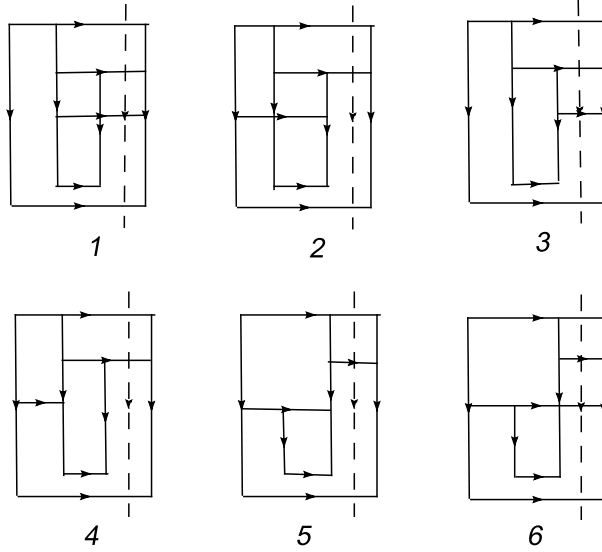


Figure 17: Feynman diagrams 3 \rightarrow 4 for the inclusive cross-section with one of the target quarks cut associated with the double cut configuration. Complex conjugate diagrams are to be added. (See notations in Fig. 4.)

In (5) we change $q_1 \leftrightarrow q_2$, $q_3 \leftrightarrow q_4$ and $k_2 \rightarrow -k_2$. In (7) we only change $q_1 \leftrightarrow q_2$. In (8) we change $q_3 \leftrightarrow q_4$ and $k_2 \rightarrow -k_2$.

Contribution from diagram (4) will be cancelled with a similar one from the single cut diagram (6) (see below).

Combining all terms and doubling we get the total DC contribution from 3 \rightarrow 4 diagrams

$$DC_{3 \rightarrow 4} = 2 \left((1) + (2) + (5) + (7) + (8) \right) = V(q_1, q_4, q_1 + k_2, q_4 - k_2) \cdot X_6, \quad (33)$$

where

$$\begin{aligned} X_6 &= \frac{1}{2} V(k_2, q_4 - k_2 | k_1 + k_2, q_4 - k_1 - k_2) \\ &+ \frac{1}{2} W(q_1 + k_2, q_2, q_4 - k_2 | q_1 + k_1 + k_2, q_2 + q_4 - k_1 - k_2) \\ &+ \frac{1}{2} W(q_2, q_1 + k_2, q_3 | q_2 + k_1, q_1 + q_3 - k_1 + k_2) \\ &- \frac{1}{2} W(q_2, q_1 + k_2, q_4 - k_2 | q_2 + k_1, q_1 + q_4 - k_1) - \frac{1}{2} W(q_1 + k_2, q_2, q_3 | q_1 + k_1 + k_2, q_2 + q_3 - k_1). \end{aligned} \quad (34)$$

We now pass to the associated single cut diagrams (SDC for 3 \rightarrow 4). Half of them with non-zero colour factors are shown in Fig. 17. The integrands are

$$(1) = \frac{1}{8} V(q_1, q_4 | q_1 + k_2, q_4 - k_2) W(q_1 + k_2, q_2, q_4 - k_2 | q_1 + q_2 + k_1 + k_2, q_4 - k_1 - k_2),$$

$$(2) = \frac{1}{8} V(q_3, q_2 | q_3 + k_2, q_2 - k_2) W(q_1, q_2 - k_2, q_4 | q_1 + q_2 + k_1 - k_2, q_4 - k_1),$$

$$(3) = -\frac{1}{8}V(q_2, q_4|q_2 + k_2, q_4 - k_2)W(q_1, q_2 + k_2, q_4 - k_2|q_1 + q_2 + k_1 + k_2, q_4 - k_1 - k_2),$$

$$(4) = -\frac{1}{8}V(q_3, q_1|q_3 + k_2, q_1 - k_2)W(q_1 - k_2, q_2, q_4|q_1 + q_2 + k_1 - k_2, q_4 - k_1),$$

$$(5^*) = -\frac{1}{4}W(q_1, q_2, q_4|q_1 + q_2 + k_2, q_4 - k_2)V(q_3, q_1 + q_2 + k_2|q_3 + k_1, q_1 + q_2 + k_2 - k_1),$$

$$(6^*) = \frac{1}{8}W(q_3, q_2, q_4|q_3 + k_2, q_2 + q_4 - k_2)V(q_3 + k_2, q_1|q_3 + k_1 + k_2, q_1 - k_1).$$

As we shall see below (6) is cancelled with a similar contribution from DC. The rest of contributions are easily transformed to the standard form. In (5) we use (22) and change $q_1 \rightarrow -q_1$ to give

$$(5) = \frac{1}{4}V(q_1, q_4|q_1 + k_2, q_4 - k_2)V(q_3, k_2|q_3 + k_1, k_2 - k_1).$$

Next we change in (2) $q_1 \leftrightarrow q_2$, $q_3 \leftrightarrow q_4$ and $k_2 \rightarrow -k_2$, in (3) $q_1 \leftrightarrow q_2$ and in (4) $q_3 \leftrightarrow q_4$ and $k_2 \rightarrow -k_2$. We obtain

$$SDC_{3 \rightarrow 4} = 2 \sum_{j=1}^5 (j) = V(q_1, q_4|q_1 + k_2, q_4 - k_2) \cdot Y_6, \quad (35)$$

where

$$\begin{aligned} Y_6 &= \frac{1}{4}W(q_1 + k_2, q_2, q_4 - k_2|q_1 + q_2 + k_1 + k_2, q_4 - k_1 - k_2) \\ &+ \frac{1}{4}W(q_2, q_1 + k_2, q_3|k_1 + k_2, q_4 - k_1) - \frac{1}{4}W(q_2, q_1 + k_2, q_4 - k_2|k_1 + k_2, q_4 - k_1 - k_2) \\ &- \frac{1}{4}W(q_1 + k_2, q_2, q_3|k_1 + k_2, q_3 - k_1) + \frac{1}{2}V(q_3, k_2|q_3 + k_1, k_2 - k_1). \end{aligned} \quad (36)$$

Finally we check that the contribution from diagram (6) cancels the similar one DC(4) from DC_{3→4}. Transformation of the integration momentum $k_2 \rightarrow q_2 + q_4 - q_3 - k_2$ transforms SDC(6) into DC(4). Since they enter the cross-section with opposite signs, they cancel in the sum.

10 Final expression for the BB inclusive cross-section

It is convenient to express the found contributions X_i and Y_i in terms of function $F(q|p) \equiv (q|p)$ defined by (9). Originally the sum of X_i and Y_i contains 114 functions F . However many terms cancel within each X_i and Y_i . After these cancellations we find non-zero X_i and Y_i in the form

$$\begin{aligned} X_2 &= -\frac{1}{4}(q_{14}|q_1 + k_1 + k_2) + \frac{1}{4}(q_1 - q_4 + k_2|q_1 + k_1 + k_2) \\ &+ \frac{1}{4}(-q_1 + q_4 - k_2|k_1 - q_1) - \frac{1}{4} + (-q_{14}|k_1 - q_1). \end{aligned} \quad (37)$$

$$\begin{aligned}
X_3 &= \frac{1}{4}(q_{14}|q_1 + k_1 + k_2) - \frac{1}{4}(q_1 - q_4 + k_2|q_1 + k_1 + k_2) \\
&\quad - \frac{1}{4}(-q_1 + q_4 - k_2| - q_1 + k_1) + \frac{1}{4}(-q_{14}| - q_1 + k_1) \\
&\quad + \frac{1}{2}\left((q_1|q_1 + k_1 + k_2) - (q_1 + k_2|q_1 + k_1 + k_2)\right) \\
&\quad - \frac{1}{2}\left((-q_1 - k_2| - q_1 + k_1) - (-q_1| - q_1 + k_1)\right). \tag{38}
\end{aligned}$$

$$\begin{aligned}
Y_2 &= -\frac{1}{2}\left(- (q_4| - q_1 + k_1) - (q_1|q_1 - k_1) + (q_{14}|k_1)\right. \\
&\quad \left.- (-q_4 + k_2|q_1 + k_1 + k_2) - (-q_1 - k_2| - q_1 - k_1 - k_2) + (-q_{14}|k_1)\right. \\
&\quad \left.+ (-q_4 + k_2| - q_1 + k_1) + (q_1|q_1 - k_1) - (q_1 - q_4 + k_2|k_1)\right) \\
&\quad + (-q_4 + k_2| - q_4 + k_1 + k_2) + (q_1|q_4 - k_1 - k_2) - (q_1 - q_4 + k_2| - k_1) \\
&\quad \quad - (q_4|q_4 + k_1) - (-k_2| - q_4 - k_1) + (q_4 - k_2| - k_1) \\
&\quad + (k_2 - q_4| - q_4 + k_1 + k_2) + (-k_2|q_4 - k_1 - k_2) - (-q_4| - k_1). \tag{39}
\end{aligned}$$

$$\begin{aligned}
X_5 &= -(q_4|q_4 + k_1 - k_2) - (-q_4 + k_2| - q_4 - k_1 + k_2) + (k_2|k_1) \\
&\quad - (-q_4 + k_2|q_1 - q_4 + k_1 + k_2) - (q_4| - q_1 + q_4 - k_1 - k_2) \\
&\quad \quad + (-q_4 + k_2| - q_1 - q_4 + k_1) + (q_4|q_{14} - k_1). \tag{40}
\end{aligned}$$

$$\begin{aligned}
X_6 &= \frac{1}{2}\left[(q_4|k_1 + k_2) - (k_2|k_1 + k_2) - (q_4 - k_2|q_4 - k_1 - k_2)\right. \\
&\quad \left.+ (q_4|q_1 + k_1 + k_2) - (-q_1 + q_4 - k_2| - q_1 + q_4 - k_1 - k_2)\right. \\
&\quad \left.+ (-q_4 + k_2| - q_1 + k_1) - (q_1 - q_4 + k_2|q_1 - q_4 - k_1 + k_2)\right. \\
&\quad \quad \left.- (q_4| - q_1 + k_1) + (q_4 + q_1|q_{14} - k_1)\right. \\
&\quad \left.- (-q_4 + k_2|q_1 + k_1 + k_2) + (-q_{14}| - q_1 - q_4 - k_1)\right]. \tag{41}
\end{aligned}$$

$$\begin{aligned}
Y_4 &= \frac{1}{4}(q_1 - q_4 + k_2| - q_4 + k_1) + \frac{1}{4}(-q_1 + q_4 - k_2| - q_1 - k_1) \\
&\quad - \frac{1}{4}(-q_{14}| - q_1 - k_1) - \frac{1}{4}(q_{14}|q_4 + k_1 - k_2). \tag{42}
\end{aligned}$$

$$Y_5 = -(q_4|q_4 + k_1) - (-q_4 + k_2| - q_4 - k_1) + (k_2| - k_1). \tag{43}$$

$$Y_6 = -\frac{1}{4}(q_4 - q_1 - k_2|q_4 - k_1 - k_2) - \frac{1}{4}(-q_4 + q_1 + k_2| - q_4 - k_1)$$

$$\begin{aligned}
& +\frac{1}{4}(q_{14}|q_4 - k_1 - k_2) + \frac{1}{4}(-q_{14}| - q_4 - k_1) \\
& +\frac{1}{2}(-q_4 + k_2| - q_4 + k_1) - \frac{1}{2}(-q_4| - q_4 + k_1) - \frac{1}{2}(k_2|k_2 - k_1). \tag{44}
\end{aligned}$$

(We recall that $q_{14} = q_1 + q_4$).

In their sum they contain 42 functions F . However more cancellations occur in the sum $\sum_i(X_i - Y_i)$. Doing this sum we finally find the total contribution to the BB cross-section from our diagrams as

$$\begin{aligned}
I_R^{BB} &= V(q_1, q_4|q_1 + k_2, q_4 - k_2) \\
&\left(-2(q_1 - q_4 + k_2|k_1) + 2(q_{14}|k_1) - 4(q_1 + k_2|k_1) + 4(q_1|k_1) \right). \tag{45}
\end{aligned}$$

It is instructive to see contributions of which diagrams survive in the final expression (45). One finds that contributions X_2 from transitions $2 \rightarrow 4$ in the D configuration Fig. 8 and Y_4 from transitions $4 \rightarrow 4$ in the single cut DC configuration Fig. 13 completely cancel. From contributions X_5 , Y_5 and Y_6 only a single diagram (plus its conjugate) gives contribution in each case, namely Fig. 14,1+3, Fig. 15,1+3 and Fig. 17,5. On the other hand for transitions SD $2 \rightarrow 4$ and DC $3 \rightarrow 4$ all diagrams in Fig. 9 and Fig. 16 respectively contribute to the final expression (45).

Cross-section I_R^{BB} is to be compared with the corresponding contribution from the KT cross-section. The latter is obtained from I^{KT} by removing one half of the first term in I_1^{KT} , since it is reproduced by I_2^{BB} , and changing sign of I_3^{KT} due to contribution I_1^{BB} , Eq. (17). So we have to compare I_R^{BB} with

$$\begin{aligned}
\tilde{I}^{KT} &= -2(k_2|k_1)(q_{14}|q_1 - k_2) + 2(q_{14}|k_2)(q_1|k_1) + 2(q_{14}|k_2)(q_4|k_1) \\
&+ 4(q_1| - k_2)(q_{14} + k_2|k_1) + 4(q_4| - k_2)(q_{14} + k_2|k_1) - 4(q_{14}| - k_2)(q_{14} + k_2|k_1) \\
&- 2(q_1| - k_2)(q_{14}|k_1) - 2(q_4| - k_2)(q_{14}|k_1) + 2(q_{14}| - k_2)(q_{14}|k_1), \tag{46}
\end{aligned}$$

where for comparison we write all 9 terms separately enumerating them as (KT1,...,KT9).

To compare the two expressions we present

$$V(q_1, q_4|q_1 + k_2, q_4 - k_2) = (q_{14}|q_1 + k_2) - (q_1| - k_2) = (q_4|k_2) \tag{47}$$

and in the term in (45) which comes from the first term in (47) shift the integration variable $k_2 \rightarrow k_2 - q_1$. Then after dropping contributions which do not depend on either q_1 or q_4 we find 10 terms

$$\begin{aligned}
I_R^{BB} &= (q_{14}|k_2) \left(-2(-q_4 + k_2|k_1) + 2(q_{14}|k_1) - 4(k_2|k_1) + 4(q_1|k_1) \right) \\
&\quad - (q_1| - k_1) \left(-2(q_1 - q_4 + k_2|k_1) + 2(q_{14}|k_1) \right) \\
&\quad - (q_4|k_2) \left(-2(q_1 - q_4 + k_2|k_1) + 2(q_{14}|k_1) - 4(q_1 + k_2|k_1) + 4(q_1|k_1) \right), \tag{48}
\end{aligned}$$

which we enumerate as (BB1,...,BB10).

We observe immediately that (BB2)=(KT9), (BB4)=(KT2)+(KT3), (BB6)=(KT7), (BB8)=(KT8). Changing in (BB5) and (BB7) $q_4 \rightarrow -q_4$ we find (KT4)+(KT5)=2(BB5)+2(BB7). Changing in (KT6) we find (KT6)= $-4(q_{14}|k_2)(k_2|k_1)$ =(BB3). Shifting in (KT1) $k_2 \rightarrow k_2 + q_1$ we have (KT1)=-2($k_2 + q_1|k_1$)($q_{14} - k_2$). Changing $k_2 \rightarrow -k_2$ and interchanging q_1 and q_4 we find (KT1)=(BB1). At this point the difference between I_R^{BB} and \tilde{I}^{KT} reduces to (BB9)+(BB10)-(1/2)[(KT4)+(KT5)]. Now we observe that shift $k_2 \rightarrow k_2 - q_1$ transforms

$$(q_1| - k_2)(q_{14} + k_2|k_1) \rightarrow (q_1|k_2)(q_4 + k_2|k_1)$$

so that the interchange $q_1 \leftrightarrow q_4$ gives (1/2)[(KT4)+(KT5)]=(BB9). So the total difference between I_R^{BB} and \tilde{I}^{KT} finally reduces to a single term (B10):

$$I_R^{BB} - \tilde{I}^{KT} = 2(q_4|k_2)(q_1|k_1) + 2(q_1|k_2)(q_4|k_1), \quad (49)$$

where we have symmetrized in q_1 and q_4 . However one can prove (see Appendix 2.) that after integration over k_2 , q_1 and q_4 with the pomeron wave functions this term vanishes. So in the end the inclusive cross-sections found in the BB and KT approaches completely coincide.

11 Conclusions

We have performed direct calculations of the inclusive cross-section for gluon production in both KT and BB approaches in the NLO. Our result shows that these cross-sections are identical. This result may look astonishing. In fact all diagrams considered for I_R^{BB} in the BB approach involve in the t -channel three or four intermediate reggeized gluons in the irreducible colorless states: the BKP states. Presence of these states together with the impossibility to use the so-called bootstrap relation due to the fixed observed gluon momentum k_1 was the reason why in [4] a very complicated equation was derived for the inclusive cross-section, which had several parts additional to the one corresponding to the KT cross-section with explicit contribution from the BKP states. Our results show that all these additional terms cancel at least in the first nontrivial order in $\alpha_s \ln s$ (and of course in the limit $N \rightarrow \infty$). Strictly speaking this does not exclude that the BKP contribution starts from the NNLO, although we think it quite improbable. In any case the comparison of the BB and KT cross-sections in the NNLO is certainly out of the question due to the scale of the corresponding calculations. So our final conclusion is that in spite of the presence of a lot of additional BKP contributions the BB and KT cross-sections are identical. This is very good news because in the opposite case one would have to calculate the BKP Green functions for their evolution, which is hardly feasible. In contrast, the KT cross-sections can be found exclusively in terms of the standard BFKL pomeron and triple pomeron vertex, which, as is well-known, even admits introduction of the running coupling.

12 Acknowledgements

The author highly appreciates discussions with J.Bartels, G.P.Vacca and especially with Yu.Kovchegov, who initiated and have kept a constant attention and interest in this work. This work was supported by grants RFFI 09-012-01327-a and RFFI-CERN 08-02-91004.

13 Appendix 1. The KT cross-section in terms of BB diagrams

The BB diagrammatic representation of the KT cross-section is just transformation to the momentum space.

The basic formula for the cross-section is [3]

$$I(y, k, b) \equiv \frac{(2\pi)^3 d\sigma}{dy d^2k d^2b} = \int d^2r P(Y - y, r) V_k(r) \left(2\Phi(y, r, b) - \Phi^2(y, r, b) \right), \quad (50)$$

where

$$V_k(r) = \frac{4\alpha_s N}{k^2} \overleftarrow{\Delta} e^{ikr} \overrightarrow{\Delta}. \quad (51)$$

The LO contribution to the inclusive cross-section on two centers comes from two sources: the quadratic term Φ^2 and the second term of the Glauber expansion of the initial target factor

$$\Phi(y - 0, r) = \Phi_0(r) - \frac{1}{2}\Phi_0^2(r).$$

So the LO contribution is

$$I_2^{LO} = -2 \int d^2r P_0(r) V_k(r) \Phi_0^2(r). \quad (52)$$

where $P_0(r)$ is the lowest order contribution to the projectile factor. Transformation to the momentum space gives

$$I_2^{LO} = -8\alpha_s N_c \int \frac{d^2q_1 d^2q_4}{(2\pi)^4} P_0(q_{14} + k) (q_{14} + k)^4 (q_{14}|k) \Phi_0(q_1) \Phi_0(q_4). \quad (53)$$

Putting the projectile and target factors to unity

$$P_0(q_{14} + k) (q_{14} + k)^4 \rightarrow 1, \quad \Phi_0(q) \rightarrow 1$$

and suppressing integration over q_1 and q_4 with weight $1/(2\pi)^2$ each we get

$$I^{LO} = -8\alpha_s N_c (q_{14}|k). \quad (54)$$

Direct calculation of the correspondibg sum of BB diagrams with V and W given by (1) and (2) correspondingly gives

$$I^{BB,LO} = -4(q_{14}|k), \quad (55)$$

which fixes the relation between the sum of all BB diagrams I^{BB} calculated with (1) and (2) and the inclusive cross-section as

$$I(y, k, b) = 2\alpha_s N_c I^{BB}. \quad (56)$$

(This confirms the relation established in a more general manner in Section 3).

In the KT cross-section contribution (55) splits into two equal parts, one of them corresponding to the second term in the Glauber expansion of the initial condition and the other to the term quadratic in Φ . They evolve differently with the BFKL kernel, so that in the NLO they become different and correspond to terms I_2^{KT} and I_3^{KT} given by (7) and (8) with the suppressed factor and integrations given by (4).

The contribution coming from the first term in (50) linear in Φ carries a twice greater coefficient. For two scattering centers it can be taken directly from the expression for the forward triple pomeron amplitude [3], which in its turn uses the normalization introduced in [6]:

$$T_{3 \rightarrow 3} = -is \frac{1}{2\pi} \int dy \int \frac{d^2 k_1}{(2\pi)^2} \frac{d^2 q_1}{(2\pi)^2} \frac{d^2 q_4}{(2\pi)^2} \Gamma(q_1, -q_1, -q_4, q_4 | k_1, -k_1) P(Y - y, k_1) P_1(y, q_1) P_4(y, q_4), \quad (57)$$

where the splitting vertex is defined according to

$$\Gamma(q_1, -q_1, -q_4, q_4 | k_1, -k_1) = \tilde{g}^2 k_1^4 \left(-\tilde{g}^2 N_c W(q_1, -q_1, q_4 | k_1, -k_1) - (2\pi)^3 \delta^2(k_1 - q_1) \left(\omega(-q_1) - \omega(-q_4) \right) - (2\pi)^3 \delta(-k_1 - q_4) \omega(-q_4) \right). \quad (58)$$

Emission from the upper pomeron implies fixing integration over one of the intermediate pomeron interaction inside, given by $-V d^2 k / (2\pi)^3$. So in the NLO we get Eq. (6), using (16), suppressing the lower legs and integration over them and doubling according to (50). The overall sign in I_1^{KT} takes into account signs of the insertion of the gluon emission operator ($-V$) and of the 3-Pomeron vertex (see [8]).

14 Appendix 2. A useful property of the BFKL pomeron

In our notation the BFKL evolution equation reads

$$\partial_y P(y, q) = \frac{g^2 N}{8\pi^3} \int d^2 \kappa \left(2(q - \kappa | q) P(y, q - \kappa) - (q | \kappa) P(y, q) \right). \quad (59)$$

We use the property that the pomeron vanishes as the two reggeized gluons are located at the same spatial point.

$$\int d^2 q P(y, q) = 0 : \quad (60)$$

Integrating Eq. (59) over q we get

$$\int d^2 q \int d^2 \kappa \left(2(q - \kappa | q) P(y, q - \kappa) - (q | \kappa) P(y, q) \right) = 0. \quad (61)$$

In the first term we shift the integration variable $q \rightarrow q + \kappa$ to obtain

$$\int d^2q \int d^2\kappa (2(q|q + \kappa) - (q|\kappa)) P(y, q) = 0. \quad (62)$$

However $(q|q + \kappa) = (q| - \kappa)$ and changing in the first term $\kappa \rightarrow -\kappa$ we find the identity

$$\int d^2q \int d^2\kappa (q|\kappa) P(y, q) = 0. \quad (63)$$

It means that apart from identity (60) one also has

$$\int d^2q \ln q^2 P(y, q) = 0. \quad (64)$$

References

- [1] M.A.Braun, Phys. Lett. **B 483** (2000) 105.
- [2] Yu.V. Kovchegov and K.Tuchin, Phys. Rev. D 65 (2002) 074026.
- [3] M.A.Braun, Eur. Phys. J **C 48** (2006) 501.
- [4] J.Bartels, M.Salvadore and G.P.Vacca, JHEP **0806** (2008) 032.
- [5] V.S.Fadin, E.A.Kuraev, L.N.Lipatov, Phys. Lett **B 60** (1975) 50;
I.I.Balitski, L.N.Lipatov, Sov. J. Nucl. Phys. **15** (1978) 438.
- [6] J.Bartels, Z.Phys. **C 60** (1993) 471;
J.Bartels, M.Wuesthoff, Z.Phys. **C 66** (1995) 157.
- [7] M.A.Braun, arxiv: 0908.3996.
- [8] M.A.Braun and G.P. Vacca, Eur. Phys. J. **C 6** (1999) 147.
- [9] J.Bartels, L.N.Lipatov and G.P.Vacca, Nucl. Phys. **B 706** (2005) 391.